

Single crystal growth and heteroepitaxy of polyacene thin films on arbitrary substrates

Hua Zhou¹, Binran Wang¹, Yiping Wang¹, Gregory P. Carpenter¹, Randall L. Headrick¹, Alex C. Mayer², Ricardo Ruiz², George G. Malliaras², and Alexander Kazimirov³

¹⁾ *Department of Physics, University of Vermont, Burlington, Vermont 05405, USA*

²⁾ *Materials Science and Engineering, Cornell University, Ithaca, New York 14853, USA*

³⁾ *Cornell High Energy Synchrotron Source, Ithaca New York, 14853, USA*

Organic molecules in the series Anthracene, Tetracene, Pentacene, are model molecules for electrical devices such as organic thin film transistors (OTFTs). A long-standing challenge in this field is to prepare single crystal films on arbitrary substrates. Here we describe two significant advances towards achieving this goal. First, we show that Anthracene thin films with single-crystal domain sizes exceeding $1 \times 1 \text{ cm}^2$ can be prepared on various substrates by a solvent deposition technique. Second, we demonstrate that highly oriented growth of Pentacene over an Anthracene film is feasible by means of organic molecular beam epitaxy (OMBE). *In situ* synchrotron x-ray scattering is used to probe the early stages of Pentacene OMBE, as well as the orientation of the Pentacene layers. Films prepared by these methods will help to explore the fundamental issues of thin film growth, as well as the limits of electric carrier transport in organic thin film devices.

Organic electronic devices have potential applications in a number of low-cost, large area electronic applications such as flat panel displays. Organic thin film transistors (OTFTs) are envisioned to drive many of these devices. Among the various materials suitable for OTFTs, Pentacene stands out as a model molecule, having the largest field effect mobility reported so far.¹⁻⁵ This has motivated a number of studies of organic semiconductor growth on dielectrics, as well as other substrates.⁶⁻¹² Recently, significant progress has been made towards fabricating high quality, large-grain, polycrystalline films of Pentacene.

In contrast to Pentacene, thin films of the related molecules Anthracene and Tetracene have received relatively little attention. In one sense this is surprising, since many fundamental advances in the field of semiconductor physics have resulted from the ability to synthesize structures from materials with similar but complementary properties. An example that comes to mind is GaAs, and related compounds such as AlAs and InAs, where alloys, superlattices, and quantum wells can be formed with exciting properties not found individually in the parent compounds. On the other hand, such structures in organic thin films may be premature given that the *best films* produced so far are merely large grain polycrystalline films. We require single crystal materials with much better properties in order to take optimal advantage of advanced structures. If it is possible to achieve true heteroepitaxial growth with single-crystal quality and sharp, stable interfaces, then the door will be opened to the exploration of more interesting

structures such as short-period superlattices and quantum wells. Potentially, many of the techniques developed for inorganic semiconductors over the past 50 years can be adopted for use in organic semiconductor materials.

In this article, we demonstrate a solvent-based method to deposit thin films of organic semiconductors, which is very general. Excellent results have been obtained for Anthracene deposition on a variety of substrates, including glass, oxidized silicon, and polymers. We find that a variety of film morphologies are formed including continuous films and separated wire-like structures with individual widths as small as a few microns. Single-crystal domains approach the length of the sample in one direction (we used samples up to 75 mm in our experiments). A practical advantage of this method is the ability to coat relatively large areas easily without resorting to a vacuum environment.

Our studies reported in this article make use of hard x-rays ($\lambda = 1.239 \text{ \AA}$) from the Cornell High Energy Synchrotron Source. Synchrotron x-ray sources offer unique advantages for structural studies of the early stages of film growth. The high intensity and excellent collimation of synchrotron x-ray beams enables studies of films down to the sub-monolayer regime.¹³⁻¹⁷

Synchrotron radiation was recently utilized to quantify the degree of ordering in Pentacene films deposited on anisotropic substrates,¹¹ and has also been applied to monitor the formation of the first two Pentacene layers on oxidized and hydrogen terminated silicon substrates.^{14,15} A study of the interface formed between silicon dioxide and Pentacene has revealed that water molecules remain at the interface when Pentacene is deposited at 10^{-6} Torr.¹⁷

Anthracene has a monoclinic structure with lattice constants $a = 8.561 \text{ \AA}$, $b = 6.036 \text{ \AA}$, $c = 11.163 \text{ \AA}$ and $\beta = 124^\circ 42'$.¹⁸ The structure is composed of layers of molecules stacked along the the c-direction with the “herringbone” packing within each layer (Fig. 1). The (001) surface has the lowest free energy, and as a result, when a thin film of Anthracene is formed the **a** and **b** lattice vectors are typically in the plane of the film. Individual molecules in the film stand nearly upright with respect to the surface, but “lean over” by an angle $\chi = (\beta - 90) = 34.6^\circ$ from the surface normal.

Anthracene films can also be used as a substrate for overgrowth of other layers. The Anthracene/Pentacene system is an excellent model system for investigating the possibility of highly oriented heteroepitaxy because of their chemical and structural similarity. Here we report

initial results for overgrowth of Pentacene. The lattice constants of Pentacene are similar to those of Anthracene, except that the value of c is significantly larger for Pentacene. This is primarily a result of the fact that the Pentacene molecule is longer. In these experiments, we are working with the so-called “thin-film” phase of Pentacene. Our own recent determination of the lattice parameters for this polymorph, which differ only slightly from other published values, are: $a = 7.58 \text{ \AA}$, $b = 5.91 \text{ \AA}$, $c = 15.42 \text{ \AA}$, and $\gamma = 90 \pm 0.2^\circ$.¹⁵ In the course of collecting the data for this paper we have also deduced that $\beta \approx 95^\circ$ for the Pentacene thin film phase. In both materials, each layer of the crystal packs into a similar herringbone structure with two molecules per unit cell, and therefore, the in-plane lattice constants are similar (figure 1). Since the natural growth direction during vapor phase growth is normal to the a - b plane, the lattice mismatch in the c -direction does not affect the lattice matching at the hetero-interface between Anthracene and Pentacene.

Vapor deposition is the standard technique to form most organic semiconductor thin films. However, we use an alternative approach for the growth of Anthracene layers, borrowed from recent research on the crystallization of synthetic spheres from a colloidal suspension.^{19,20} It has been shown that strong capillary forces at the meniscus between a substrate and a colloidal suspension of spherical particles can induce crystallization into a nearly two-dimensional array

of controllable thickness.²⁰ If this meniscus is slowly swept across a vertically placed substrate by solvent evaporation, thin two-dimensional opals can be deposited.

We have discovered that the process described above is also an effective method for the growth of planar organic crystals from solution. In one trial run, a glass microscope slide was placed vertically in a vial containing a solution of Anthracene in ethyl acetate. As the solution slowly evaporated, the meniscus of the solution was swept across the surface towards the lower edge of the slide, depositing a thin film of Anthracene. The film produced by this method is colorless and perfectly transparent. Figure 2 shows a photograph of the film viewed through crossed polarizers with illumination from behind the sample. The Anthracene film induces a large rotation of the polarization producing the contrast. As a result, a clear pattern of domains becomes visible that were not readily apparent under normal room lighting.

Control over the thickness and morphology of films can be achieved by varying the concentration of the solution. However, we have chosen a more novel method to vary the structure of our films. Draining or pumping away the solvent at a controlled rate achieves direct control over the *in-plane* growth rate. This typically produces films with submicron thickness

for in-plane growth rates larger than 1 cm/hr. Note that this method does not provide direct control of the *thickness* of the film, although the general trend is towards thinner films for higher pumping speeds. Also, films become discontinuous for higher in-plane growth rates. For example, figure 3 shows a fluorescence micrograph of an Anthracene film deposited at ~5 cm/hr. The bright areas are Anthracene and the dark areas are the silicon underneath. The image shows that an unexpected two-dimensional dendritic structure is formed. Additional imaging by polarized light microscopy showed that the crystallographic orientation is the same over the entire area shown ($1 \times 1.25 \text{ mm}^2$).

The apparent mechanism that forces the selection of the highly oriented domains shown in Figures 2 and 3 is rather interesting. Small nuclei form early in the process and become elongated as the liquid level is lowered down the surface of the substrate. A preferred crystallographic direction is selected, since crystallites grow faster in certain low-index growth directions. Slow-growing nuclei with unfavorable orientations are left behind as the process proceeds, and the fast-growing domains increase rapidly in width, eventually squeezing out less favored orientations. The end result is the domain structure shown in figure 2, where single-crystal domains stretch almost the entire length of the surface in the growth direction, and may exceed one centimeter in the transverse direction. Adjacent domains have similar orientations, lying within a range of approximately $\pm 10^\circ$. The mechanism is similar to the one proposed to

explain recent observations of grain growth in ion beam assisted deposition of inorganic thin films, where faster growing grains with preferred crystallographic orientations overtake and shadow slower-growing domain orientations.²¹

Figure 4 shows the results of an x-ray diffraction θ - 2θ scan of the sample shown in figure 3. Six orders of $(00l)$ reflections are clearly observed, indicating that the film is of good quality with the c^* reciprocal lattice axis oriented normal to the surface. A layer spacing of $d = 9.18 \text{ \AA}$ was derived from this scan, which is consistent with the known crystal structure of bulk Anthracene. A small piece of this sample was mounted in a custom-built evaporation chamber coupled to an x-ray diffractometer for Pentacene evaporation as described in the methods section.²² X-ray diffraction scans performed *in-situ* during the deposition of Pentacene are shown in figure 5. The Pentacene (001) and (002) reflections gradually sharpen and increase in intensity, in the characteristic of laminar growth. The positions of the reflections correspond to a layer spacing of $d = 15.4 \text{ \AA}$, in good agreement with the established value for the “thin film” phase of Pentacene. Growth of Pentacene was stopped at approximately 6 monolayers.

Grazing incidence x-ray diffraction scans were performed on additional Anthracene films and Anthracene films with Pentacene overlayers, in order to establish the in-plane orientation of both layers. A sample prepared in the same manner as Fig. 3, with a 40 nm thick Pentacene overlayer exhibited a planar, oriented dendritic surface morphology and was found to be predominantly (>95%) single crystal by polarization microscopy. Figure 6 shows an azimuthal scan on the (200) reflection of Anthracene (red-filled circles) for this sample. If the film were polycrystalline, composed of domains with a perfectly random distribution of azimuthal orientations, a continuous low intensity would be observed. Since we observe one dominant reflection at 0° , the film is predominantly single-crystal. However, the left inset shows evidence for two grains with $\sim 1^\circ$ misorientation relative to each other.

In order to assist the reader in interpreting the orientations of the Anthracene and Pentacene crystal planes in our aligned samples, we have included a stereographic projection as an inset to Fig. 6. The polar angle between the (001) reflection and the (200) reflection is $\beta^* = 180 - \beta$, where β is the real-space angle between the **a** and **c** lattice vectors of the thin-film crystal structure, and β^* is the corresponding polar angle in the stereographic projection. The Anthracene (200) is observed at $\beta^* = 55.4^\circ$, consistent with the structure of Anthracene.¹⁸ The path of the scan corresponding to the Anthracene (200) data shown in Fig. 6 is indicated in the inset by the red dashed line.

An additional piece of information about the Anthracene film can be obtained from Figure 6: We have oriented the sample so that the scattering vector is perpendicular to the film growth direction at the azimuthal angle $\phi=0$. Therefore, since the (200) reflection appears at $\phi=0$, we conclude that the [200] direction is perpendicular to the Anthracene growth direction. In other words the domains shown in Figures 2 and 3 are oriented with their long axes parallel to the [010] crystallographic direction.

The data of Fig. 6 confirm that the individual planar dendrites in fig. 3 have identical crystallographic orientations. Apparently, a combination of the preferred orientation imposed by the deposition process, and the links between adjacent branches in the structure is enough to select a single crystallographic orientation for the whole area. We do not fully understand the origin of this two-dimensional dendrite structure, but it is likely related to well-known growth instabilities such as the Mullins-Sekerka instability,²³ which may be induced by concentration gradients as molecules diffuse in the region of the meniscus and are depleted by incorporated into the film.

Figure 6 also shows a scan for the (200) reflection of Pentacene on the same sample (blue triangles), which exhibits strong reflections with a continuous low intensity in-between. The Pentacene (200) reflection is completely separated from the Anthracene (200) because of different tilt of molecules, and hence of the unit cell. As a result of this difference, the Pentacene (200) is observed at $\beta^* = 85^\circ$, which directly gives $\beta = 95^\circ$ for the thin film phase of Pentacene. The path of the scan corresponding to the Pentacene (200) data is indicated in the inset by the blue dashed line. The background level for the Pentacene scan is about 1000 counts, so the fact that the intensity between the reflections is higher than 1000 indicates that there are some misoriented grains. Since the sample has a discontinuous structure with regions of the substrate visible (Fig. 3), it is reasonable that some fraction of the Pentacene film grows in a polycrystalline mode, hence the presence of the observed continuous ring in reciprocal space. The dominant aligned peaks are correlated with the growth direction of the Anthracene base layer, and also with the Anthracene crystallographic orientation. The reflection at $\phi = \pm 180^\circ$ is attributed to a crystal orientation with the [200] direction pointing in the opposite direction. Based on this information, we find that the preferred Anthracene/ Pentacene epitaxial relationship is $(001)_a \parallel (001)_p$ and $[100]_a \parallel [100]_p$.

We have not observed strain effects on Pentacene layers. Rather, all of the observed reflections, including (001), (200), (020), and (110) appear to be at their unstrained positions.

This may be interpreted as evidence of incommensurate epitaxy. On the other hand, the ratios of the Anthracene and Pentacene lattice parameters fall very close to the rational fractions $9/8$ (within 0.3%) and $51/50$ (within 0.1%). When the ratios are rational numbers, the growth is classified as “coincident epitaxy”, where every n th site of the substrate lattice is coincident with every m th site of the overlayer’s lattice, and n, m are integers.²⁴ This might help to explain the high degree of azimuthal orientation observed for Pentacene growth on Anthracene, since the coincidence effect would reduce the interface energy between the layers relative to random orientations. There is also a possibility of strain effects during the initial stages of nucleation and growth of the Pentacene films that have relaxed by the time the film reaches its final thickness. If the film were fully coherent during the initial stages of nucleation, then the orientation would be determined at that time. Another effect that can cause oriented epitaxy is orientation by surface features such as step-edges or facets. Presently, we do not know which of these effects is the dominant one.

Previous work has shown that transistors fabricated from oriented Pentacene films have higher mobility than randomly oriented films.^{11,12} For example, Swiggers et al., find that for Pentacene film deposited onto rubbed polymers, 27% of the film is within a 30° range in azimuth. This ordering leads to a factor of 2.5 improvement of thin-film-transistor saturation current.¹¹ Therefore, even a modest degree of ordering can lead to OTFT’s with significantly

improved properties. From figure 6, we estimate that approximately 50% of the film is ordered, and the widths of the reflections are about 10° . Since the Anthracene layer is discontinuous, randomly oriented Pentacene grains have probably formed in areas where the bare oxidized-silicon substrate is not covered by the Anthracene layer, which would cause us to underestimate the ordered fraction of Pentacene deposited onto Anthracene.

In conclusion, we have demonstrated growth of Anthracene thin films with macroscopic single-crystal domain sizes. The deposition method is very general, and may be extended to the growth of other materials. Pentacene grows as a highly oriented film on top of the Anthracene, and maintains the crystallographic orientation of the Anthracene layer. The observed high-degree of ordering is somewhat surprising, since there is a significant degree of lattice mismatch between the two materials, and the interface interaction between the two materials is very weak. Given this positive result, we believe that a large number of other organic epitaxial systems will ultimately be discovered. Both of the advances reported here may spur the exploration of new physical phenomena, and the development of novel or improved organic electronic devices based on advanced structures.

Methods

Anthracene thin film preparation

Anthracene films were deposited from a 50% saturated solution of Anthracene in ethyl acetate. Two variations of the film deposition method were used: (i) A 75 mm by 25 mm sample of glass or silicon was placed upright in a staining jar (Krackeler Scientific Inc.) containing the solution. The staining jars hold four samples upright simultaneously. The solution was allowed to evaporate over a period of 8 – 12 hours. (ii) A 600 mL beaker was used as a container, and an oxidized silicon sample was suspended upright using a fixture to hold the sample from the top. A peristaltic pump (Rainin Instrument Co. Inc.) was used to gradually reduce the solution level at a controlled rate of 1 – 5 cm/hr. All samples were subsequently examined with an optical microscope (Zeiss Axioskop), using fluorescence microscopy and polarized-light microscopy, with illumination from a mercury lamp. Selected samples were examined with x-ray diffraction as described in the main text.

Pentacene thin film preparation

Pentacene films were prepared in a custom-built vacuum evaporator,²² which was mounted in a four-circle x-ray diffractometer at the A2 station of the Cornell High Energy Synchrotron Source (CHESS). Substrates consisted of (100) p-type silicon wafers with a native oxide and an

Anthracene film, prepared by method (ii) above. Pentacene was evaporated from a tantalum boat under vacuum of 10^{-6} Torr and a substrate temperature of -15° C. The rate of deposition was 0.1 – 0.5 nm/min, as measured by a quartz crystal microbalance (QCM). The QCM was calibrated using AFM measurements in sub-ML thick films. Film growth was monitored during deposition at CHESS by using 10.0 keV x-rays ($\lambda = 1.239 \text{ \AA}$) with a flux of $\sim 10^{13}$ photons/sec, incident to the sample through a Be window. X-ray measurements were performed *in-situ* without breaking vacuum. A scintillation counter was used for measuring the scattered x-ray intensity.

References

- ¹Dimitrakopoulos, C.D. & Malenfant, P.R.L. "Organic thin film transistors for large area electronics," *Advanced Materials* **14**, 99-117 (2002).
- ²Lin, Y.-Y., Gundlach, D.J., S.F. Nelson, S.F. & Jackson, T.N. "Stacked Pentacene layer organic thin-film transistors with improved characteristics," *IEEE Elect. Dev. Lett.* **18**, 606-8 (1997).
- ³Halik, M., *et al.* "High-mobility organic thin-film transistors based on α,α' -didecyloligothiophenes," *J. Appl. Phys.* **93**, 2977-81 (2003).

- ⁴Bonse, M., Thomasson, D.B., Klauk, H., Gundlach, D.J. & Jackson, T.N. “Integrated a-Si:H/Pentacene inorganic/organic complementary circuits,” International Electron Devices Meeting 1998 , 249-52 (1998).
- ⁵Dodabalapur, A., Torsi, L. & Katz, H.E. “Organic Transistors: Two-Dimensional Transport and Improved Electrical Characteristics,” Science **268**, 270-271 (1995).
- ⁶Forrest, S.R., Burrows, P.E., Haskal, E.I. & So, F.F. “Ultrahigh-vacuum quasiepitaxial growth of model van der Waals thin films II. Experiment,” Phys. Rev. B (Condensed Matter) **49**, 11309-21 (1994).
- ⁷Biscarini, F., Zamboni, R., Samon, P., Ostojia, P. & Taliani, C. “Growth of conjugated oligomer thin films studied by atomic-force microscopy,” Phys. Rev. B (Condensed Matter) **52**, 14868-77 (1995).
- ⁸Fenter, P., Schreiber, F., Zhou, L., Eisenberger, P. & Forrest, S.R. “In situ studies of morphology, strain, and growth modes of a molecular organic thin film,” Phys. Rev. B. (Condensed Matter) **56**, 3046-53 (1997).
- ⁹Brinkmann, M., Biscarini, F., Taliani, C., Aiello, I. & Ghedini, M. “Growth of mesoscopic correlated droplet patterns by high-vacuum sublimation,” Phys. Rev. B (Condensed Matter) **61**, R16339-42 (2000).
- ¹⁰Durr, A.C. *et al.* “Rapid roughening in thin film growth of an organic semiconductor (diindenoperylene),” Phys. Rev. Lett. **90**, 016104/1-4 (2003).

- ¹¹Swiggers, M.L. *et al.* "Orientation of Pentacene films using surface alignment layers and its influence on thin-film transistor characteristics," *Appl. Phys. Lett.* **79**, 1300-2 (2001).
- ¹²Brinkmann, M. *et al.* "Orienting tetracene and Pentacene thin films onto friction-transferred poly(tetrafluoroethylene) substrate," *J. Phys. Chem. B* **107** (38), 10531-9 (2003).
- ¹³Ruiz, R. *et al.* "Dynamic scaling, island size distribution, and morphology in the aggregation regime of submonolayer Pentacene films," *Physical Review Letters* **91** (13), 136102/1-4 (2003).
- ¹⁴Ruiz, R. *et al.* "Pentacene ultrathin film formation on reduced and oxidized Si surfaces," *Physical Review B: Condensed Matter* **67** (12), 125406/1-7 (2003).
- ¹⁵Ruiz, R. *et al.* "Structure of Pentacene thin films," *Appl. Phys. Lett* **85** (21), 4926-8 (2004).
- ¹⁶Fritz, S.F., Martin, S.M., Frisbie, C.D., Ward, M.D. & Toney, M.F. "Structural characterization of a Pentacene monolayer on an amorphous SiO₂ substrate with grazing incidence x-ray diffraction," *J. Am. Chem. Soc.* **126**, 4084 (2004).
- ¹⁷Mayer, A.C., Ruiz, R., Headrick, R.L., Kazimirov, A. & Malliaras, G.G. "Early stages of Pentacene film growth on silicon oxide," *Organic Electronics* **5** (5), 257-263 (2004).
- ¹⁸Mathieson, A.L., Robertson, J.M. & Sinclair, V.C. "The Crystal and Molecular Structure of Anthracene. I. X-ray Measurements," *Acta. Cryst.* **3**, 245 (1950).
- ¹⁹Denkov, N.D. *et al.* "Two-dimensional crystallization," *Nature* **361**, 26 (1993).

- ²⁰Vlasov, Y.A., Bo, X.-Z., Sturm, J.C. & Norris, D.J. “On-chip natural assembly of silicon photonic bandgap crystals,” *Nature* **414**, 289 (2001).
- ²¹Dong, L. & Srolovitz, D.J. “Texture development mechanisms in ion beam assisted deposition,” *J. Appl. Phys.* **84** (9), 5261-9 (1998).
- ²²Headrick, R.L., Malliaras, G.G., Mayer, A.C., Deyhim, A.K. & Hunt, A.C. “Development of a Compact System for In-situ X-ray Scattering Studies of Organic Thin Film Deposition,” in the proceedings of the Eighth International Conference on Synchrotron Radiation Instrumentation, (eds. Warwick, T., Arthur, J., Padmore, H.A., & Stohr, J.) **705**, 1150 (American Institute of Physics Conference Proceedings, San Francisco, CA. 2003).
- ²³Pimpinelli, A. & Villain, J. *Physics of Crystal Growth* (Cambridge University Press, 1998).
- ²⁴Hooks, D.E., Fritz, T. & Ward, M.D. “Epitaxy and Molecular Organization on Solid Substrates,” *Adv. Mater.* **13** (4), 227-241 (2001).

Acknowledgements This research was supported through the CAREER program of the National Science Foundation, and through the Cornell Center for Materials Research, a Materials Research Science and Engineering Center of the National Science Foundation. The National Science Foundation also supports the Cornell High Energy Synchrotron Source.

Competing Interests statement The authors declare that they have no competing financial interests.

Correspondence and requests for materials should be addressed to R.L.H. (rheadrick@uvm.edu).

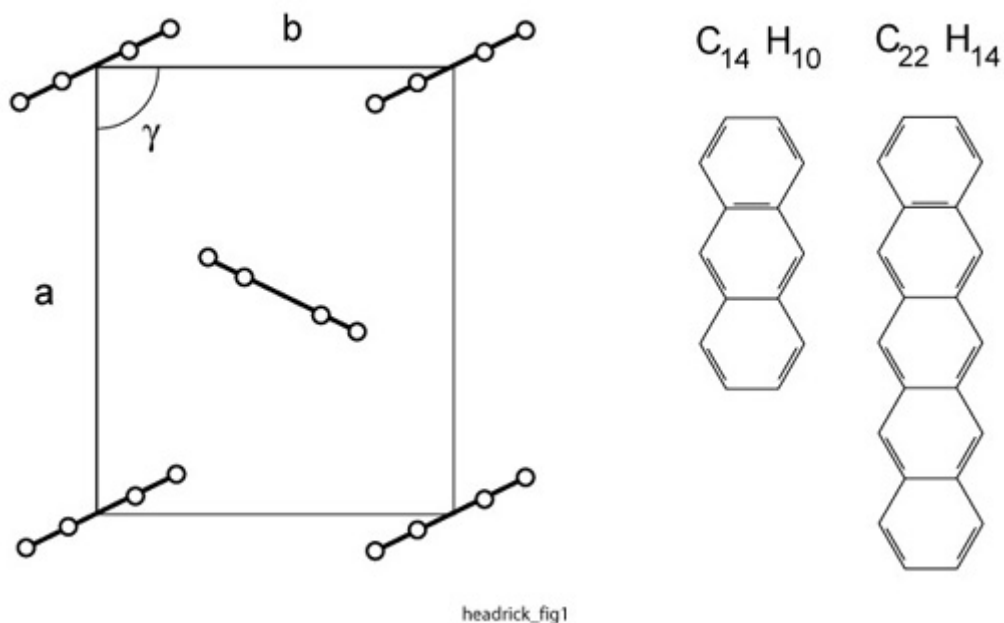


Figure 1. Schematic representation of the herringbone packing of Anthracene ($C_{14}H_{10}$) and Pentacene ($C_{22}H_{14}$) looking down along the c -axis. The packing within layers is similar for the two materials, with the long axis of the molecule oriented along the c -axis, which is directed out of the page in the diagram. The lattice parameter mismatches between the bulk phase of Anthracene and the “thin film” ($d = 15.4 \text{ \AA}$) phase of Pentacene are $\Delta a/a = 12.3\%$, and $\Delta b/b = 2.1\%$.

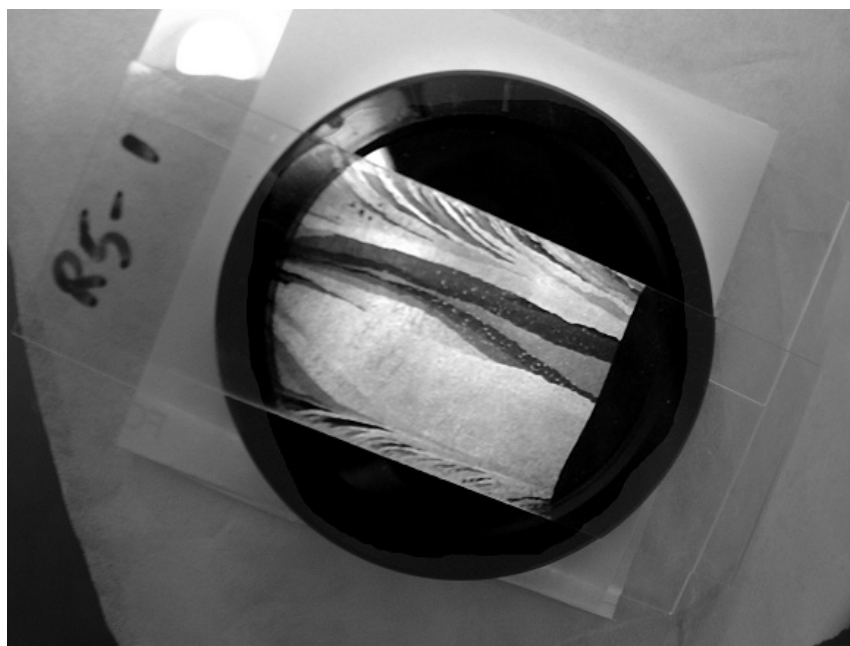


Figure 2. Unmagnified photograph of an Anthracene thin film deposited on a 75 mm by 25 mm glass slide viewed through crossed polarizers. The light source is behind the sample, followed by the first polarizer (the black disk visible in the image), and the sample itself. The domain structure of the film is visible, with a grain size exceeding one centimeter in some areas of the film. The domains are much longer along the growth direction, which is along the long direction of the slide. Rotation of the sample by 45° reverses the contrast.

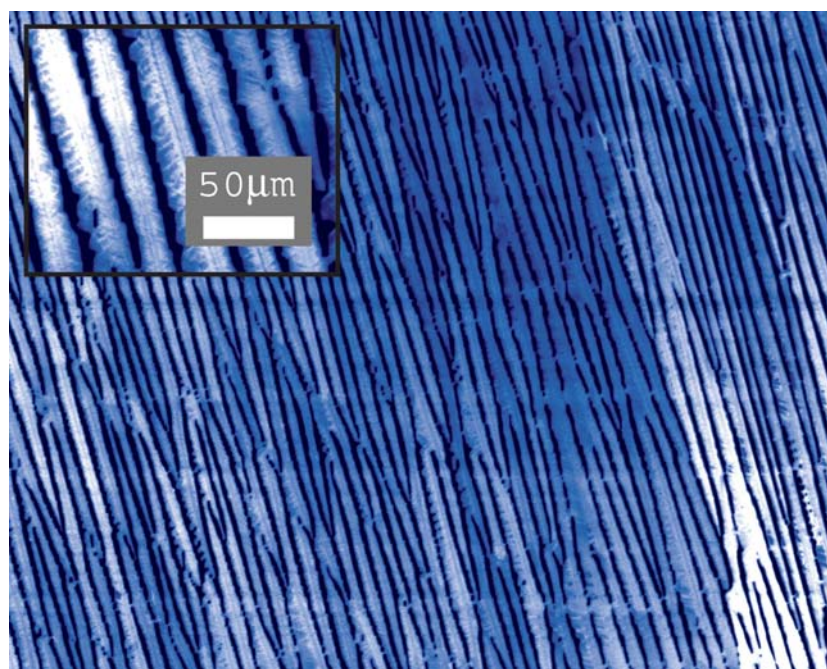


Figure 3. Fluorescence micrograph of single crystal Anthracene deposited on an oxidized silicon surface. During the growth of this film, the meniscus of the solvent was swept towards the bottom of the image. Two-dimensional dendritic structures are observed, which are nearly aligned with the nominal growth direction. Faint horizontal features are observed in the image, which mark the position of the solvent's meniscus at several points during the growth process. They are probably the result of vibration or air currents, which tend to disturb the surface of the solvent. The image area is $1 \times 1.25 \text{ mm}^2$, and the inset shows an enlarged view of the same image.

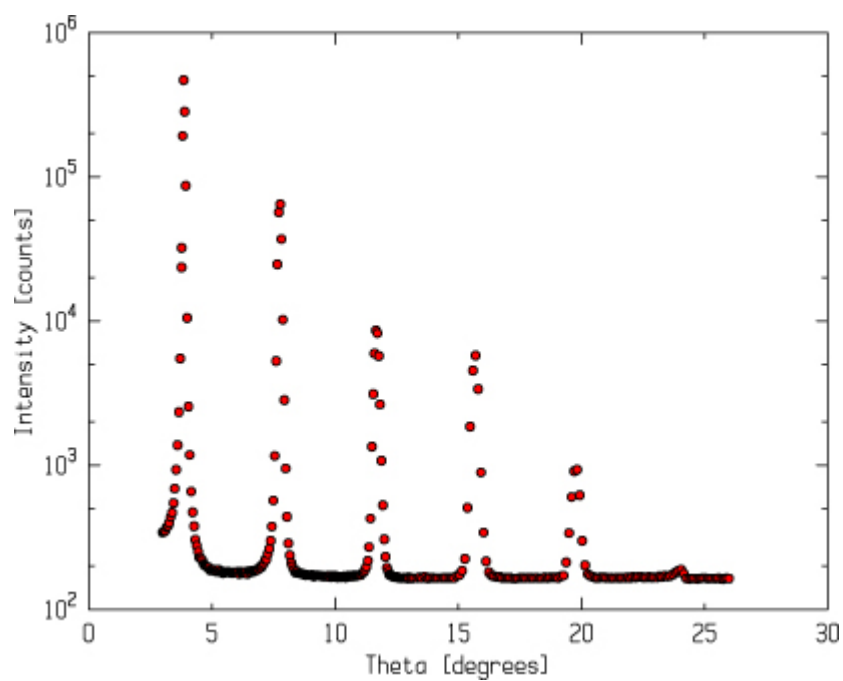


Figure 4. Specular x-ray scan of an Anthracene thin film deposited on an oxidized silicon wafer. Six orders of (00L) reflections are observed.

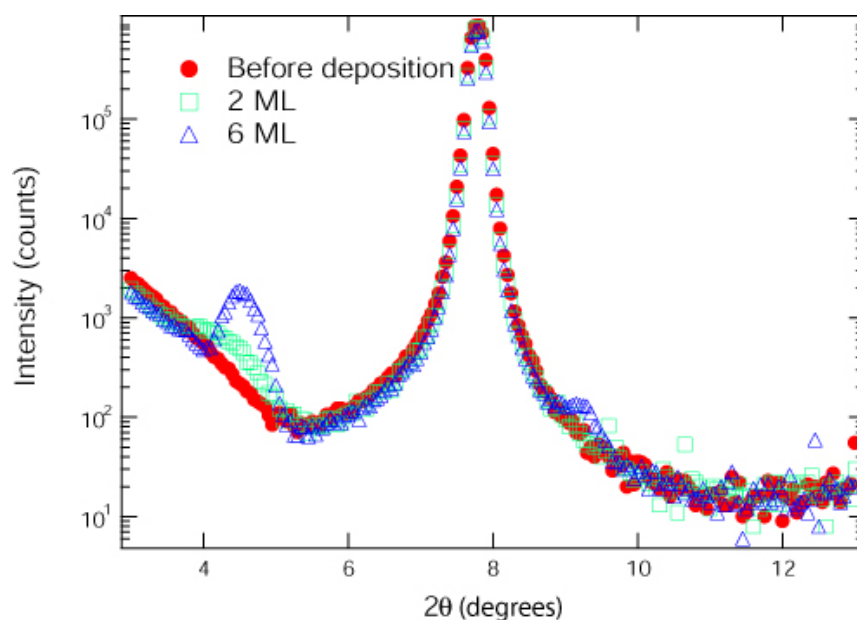


Figure 5. Specular x-ray scans through the Anthracene (001) reflection compared with and without a Pentacene epilayer. Three scans are shown for the sample before, Pentacene deposition (red-filled circles), after deposition of 2 monolayers of Pentacene (green squares), and after 6 monolayers of Pentacene (blue triangles). The positions of the Pentacene reflections are consistent with the $d = 15.4 \text{ \AA}$ phase, which is commonly observed for very thin films of Pentacene.

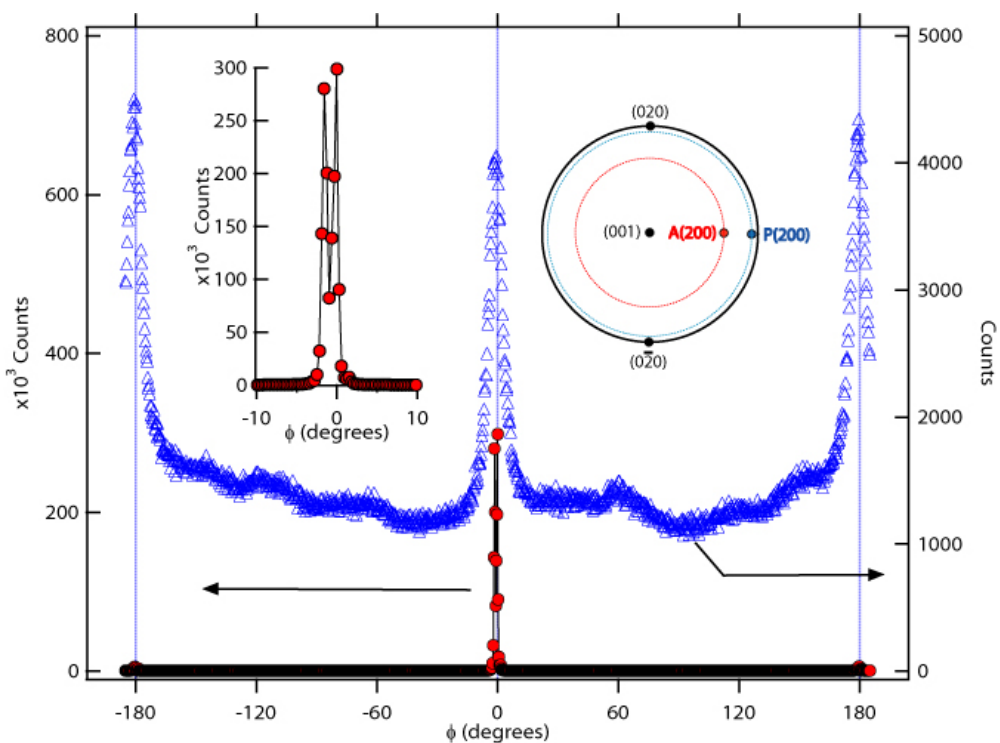


Figure 6. X-ray diffraction (200) azimuthal scans. Data are shown for the Anthracene (200) reflection (red-filled circles), and the Pentacene (200) reflection (blue triangles) through 360° . The dominant Anthracene crystal orientation results in reflection at $\phi = 0^\circ$, while Pentacene shows reflections at 0 and 180° . The left inset shows an expanded view of the Anthracene data near $\phi = 0^\circ$, revealing two peaks separated by 1° . The right inset shows a stereographic projection, depicting the azimuthal and polar angles of each reflection, and the paths of the azimuthal scans for each set of data shown.